

The vicinity of the Earth-Moon L_1 point in the Bicircular Problem*

Àngel Jorba, Marc Jorba-Cuscó and José J. Rosales
Departament de Matemàtiques i Informàtica
Barcelona Graduate School of Mathematics (BGSMath)
Universitat de Barcelona (UB)
Gran Via de les Corts Catalanes 585, 08007 Barcelona, Spain
E-mails: angel@maia.ub.es, marc@maia.ub.es, rosales@maia.ub.es

April 2nd, 2019

Abstract

The Bicircular model is a periodic time dependent perturbation of the Earth-Moon Restricted Three-Body problem that includes the direct gravitational effect of the Sun on the infinitesimal particle. In this paper we focus on the dynamics in the neighbourhood of the L_1 point of the Earth-Moon system. By means of a periodic time dependent reduction to the centre manifold, we show the existence of two families of quasi-periodic Lyapunov orbits, one planar and one vertical. The planar Lyapunov family undergoes a (quasi-periodic) pitchfork bifurcation giving rise to two families of quasi-periodic Halo orbits. Between them, there is a family of Lissajous quasiperiodic orbits, with three basic frequencies.

*This work has been supported by the grants MTM2015-67724-P and 2017 SGR 1374. The project leading to this application has received funding from the European Union's Horizon 2020 research and innovation programme under the Marie Skłodowska-Curie grant agreement #734557.

Contents

1	Introduction	3
1.1	The L_1 point	4
1.2	Normalizing transformations	5
2	Normal forms for periodic time dependent Hamiltonians	6
2.1	The symplectic Floquet Theorem	6
2.2	Higher order normal form	9
2.3	Centre manifold reduction	10
2.4	Changes of variables	11
2.5	Complexification and realification	11
3	The dynamical replacement of L_1 in the BCP	12
3.1	The dynamical equivalent of L_1	12
3.2	The Floquet change	12
3.3	On the expansion of the Hamiltonian	13
4	Dynamics near L_1 in the BCP	14
4.1	Dynamics in the centre manifold	15
4.2	Halo and Lissajous orbits	17
5	Conclusions and future work	20
A	Appendix: Details on the implementation	20
A.1	On Taylor-Fourier series	21
A.1.1	The arithmetic of Fourier Series	21
A.1.2	Handling Homogeneous Polynomials	22
A.2	On the implementation of the Floquet transformation	23
A.3	Testing the software	24
	References	24

1 Introduction

The motion of a test particle in the proximity of Earth and Moon is a hot topic in astrodynamics. The list of potential applications that could benefit from a deeper understanding of the natural dynamics near Earth and Moon is long and it is increasing day by day. Let us mention, for instance, the possibility of setting an extraterrestrial hub, the exploration in-situ of natural resources, deep space exploration by means of telescopes, new solutions for the delicate issue of space debris, end-of-life strategies adapted to the natural dynamics and, probably the most recent examples, the study of mini-moons, small objects captured (temporarily) by the Earth.

The simplest model that describes the motion of a small particle in the Earth-Moon system is the Restricted Three Body Problem (RTBP). The very specific properties of the Earth-Moon system, such as the large mass ratio between Moon and Earth; the eccentricity of the motion of the primaries or the uniformly large effect of Sun’s gravity, are certainly not well captured by the Earth-Moon RTBP. It is natural, therefore, to look for a more sophisticated model. Sun’s gravitational acceleration upon the test particle is one of the most relevant forces ignored by the RTBP, at least if a large vicinity of Earth and Moon is considered. This effect is called direct effect of Sun’s gravity. There is, however, another effect of Sun’s gravity on the particle, the indirect one: the gravity of Sun changes the motion of Earth and Moon, therefore the motion of the test particle suffers a small deviation according to the new trajectories of Earth and Moon. This effect is especially important near Earth and Moon. This work does not consider the indirect effect.

To write the equations of motion, it is usual to take the same units and reference frame as in the RTBP: The origin is taken at the centre of mass of Earth and Moon, and the axis are rotating such that Earth and Moon are sitting on the x axis. Then, Sun is moving around the origin in a circular way (see Figure 1). Defining the momenta as $p_x = \dot{x} - y$, $p_y = \dot{y} + x$ and $p_z = \dot{z}$, the motion of the infinitesimal particle is described by a Hamiltonian system that depends on time in a periodic way:

$$H_{BCP} = \frac{1}{2} (p_x^2 + p_y^2 + p_z^2) + yp_x - xp_y - \frac{1-\mu}{r_{PE}} - \frac{\mu}{r_{PM}} - \frac{m_S}{r_{PS}} - \frac{m_S}{a_S^2} (y \sin \theta - x \cos \theta),$$

where $r_{PE}^2 = (x - \mu)^2 + y^2 + z^2$, $r_{PM}^2 = (x - \mu + 1)^2 + y^2 + z^2$, $r_{PS}^2 = (x - x_S)^2 + (y - y_S)^2 + z^2$, $x_S = a_S \cos \theta$, $y_S = -a_S \sin \theta$, and $\theta = \omega_S t$ (see Table 1 for the values of the parameters). The Bicircular Problem (BCP) is among the simplest models considering the gravitational effects of Earth, Moon and Sun on a test particle. This model was introduced in [Hua60, CRR64]. In the BCP Earth and Moon move as in the RTBP, and Earth-Sun barycentre and Sun move in circular orbits around their centre of mass. Note that this motion does not follow Newton’s laws, since we are not taking into account the effect of Sun on the motion of Earth and Moon. In fact, this model can be regarded as the coupling of two RTBP. The BCP is a periodically time

μ	=	0.012150581623433623	m_S	=	328900.549999999906
ω_S	=	0.925195985518289646	a_S	=	388.81114302335106

Table 1: Floating point values used for the different constants of the BCP.

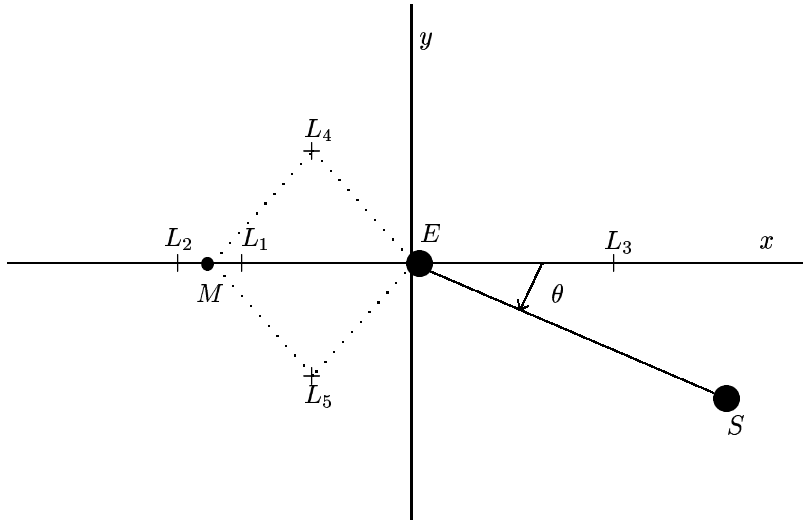


Figure 1: Sketch of the Bicircular problem. The points $L_{1,\dots,5}$ are the Lagrangian (equilibrium) points of the Earth-Moon RTBP. They are not equilibrium points of the BCP due to the effect of the Sun.

dependent Hamiltonian system, that can be seen as a periodic time dependent perturbation of the RTBP. For instance, it is well known that, near the triangular points, the phase space is qualitatively changed by the effect of Sun, see [GJMS91, SGJM95, CJ00, Jor00].

1.1 The L_1 point

The objective of this work is to describe the dynamics of the BCP in an extended neighbourhood of L_1 . As the BCP is a periodic perturbation of the RTBP, the Lagrangian points of the RTBP are no longer equilibria, and they are replaced by periodic orbits with the same period as the perturbation. These periodic orbits are usually called dynamical equivalents of the equilibria. Henceforth, the goal of this work is to understand the dynamics in a neighbourhood of the dynamical equivalent of L_1 .

It is well known that the L_1 point of the RTBP is very unstable. This character is inherited by the BCP, and the monodromy matrix around the periodic orbit that replaces L_1 in the BCP has an hyperbolic eigenvalue close to 4.287×10^8 . This makes extremely difficult to study the existence of periodic and quasi-periodic solutions by means of numerical simulations. Therefore, we will introduce a sequence of transformations to separate the hyperbolic behaviour from the non-hyperbolic one. As we will see, this process reduces the Hamiltonian system in one degree of freedom. This reduced Hamiltonian does not have the hyperbolic behaviour mentioned above so it can be studied by means of standard numerical methods. The obtained information can be transported to the initial system by means of a change of variables.

A natural approach for these simplifying transformations is to use some kind of normal form. The idea is to modify the system by means of changes of variables to make it more simple in some determined sense. In dynamical systems and, in particular, Hamiltonian dynamics, normal forms play an important role, indeed, they stood out as a tool to tackle a number of problems, especially in celestial mechanics, see, for instance [GDF⁺89, GG78, GG85, JS94, Sim89, Sim98].

1.2 Normalizing transformations

Let us suppose that we want to describe the motion around some periodic orbit of period T of a T -periodic time dependent Hamiltonian system. By means of a translation, we can move the periodic orbit to the origin of coordinates. That is, we perform a (periodic) change of variables that fixes the trajectory of the periodic orbit at the origin of the new coordinates so that now the origin is an equilibrium point of a time dependent Hamiltonian system. Therefore, the power expansion of the Hamiltonian at the origin does not have terms of first order.

The linear normal behaviour around the origin (i.e., the periodic orbit) is determined by the variational flow. The eigenvalues of the monodromy matrix, that is, the solution of the first order variational equations evaluated at the time T , define the stability of the origin (i.e. of the periodic orbit). This linear behaviour is also given by the second order terms of the Hamiltonian expanded around the orbit. We can use the classical Floquet Theorem to cast the second order of the Hamiltonian to constant coefficients. Also, we can choose coordinates for which the elliptic and hyperbolic directions are decoupled. This is known as the Floquet (linear) Normal Form.

The hyperbolic part can be used to understand several phenomena in dynamics (for instance, connections between a neighbourhood of L_1 and other parts of the phase space) but this is not our goal here. To skip the hyperbolic part, it is useful to do a change of variables to uncouple, up to a given order, the hyperbolic part and the central part in order to focus on the bounded motion around the periodic orbit. In the literature, this process is called centre manifold reduction. Most of the references are concerned with centre manifold reduction around equilibrium points of autonomous systems, see [Jor99, JM99, Sim96]. There are also some works for periodic time dependent situations, see [GJMS93, SGJM95, GJ01] for studies on the triangular points based on normal form computations. The approximation of centre manifolds for the L_2 point has been considered in [And98, AS00, And02]. Let us mention as well a couple of works on normal forms for quasi-periodic time dependent Hamiltonians, [GJL05, GJ05].

There are two different approaches to deal with centre manifolds. The first, the ones we use in this work, is to perform a number of canonical changes of variables to uncouple, up to high order, the hyperbolic part and have a relatively simple way to describe the centre motion by fixing the hyperbolic coordinates. Sometimes, this is called normal form style. Another strategy is to compute a parametrization of the manifold. The classical graph transform method [FJ10] and the more general and powerful parametrization method [BMGLD17] allow to compute expansions of these parametrization up to high order.

As we have mentioned, the approach here is to use a Hamiltonian normal form, that is, the changes of variables are not performed on the vectorfield, but on the Hamiltonian function. This has the advantage of reducing the number of expressions we have to deal with from $2n$ differential equations to one Hamilton function. The disadvantage is that all changes of variables must be canonical. It is not trivial to produce explicit nonlinear canonical changes and, among the methods to obtain such transformations, we have chosen the Lie series method.

This paper is structured as follows, in Section 2 we review how to adapt the classical Lie series method to the case of Hamiltonian systems that depend periodically on time. We discuss how to compute generating functions to fulfil distinct purposes. In particular, we explain how construct generating functions that, besides removing certain monomials, also removes time dependence. In Section 3 we study the periodic orbit that replaces L_1 in the BCP. We discuss the linear normal behaviour of the orbit and discuss the computation of the Floquet normal form. We explain, as well, how to compute the expansion of the Hamiltonian of the BCP around the

periodic orbit that replaces L_1 . In Section 4 we analyse the dynamics in the center manifold. As the time dependence has been removed, we are able to reduce the problem of describing the dynamics in the centre manifold by fixing an energy level and using suitable Poincaré sections. This reduces the study to the visualisation of a family of Area Preserving Maps, parameterized by the energy level. We classify the different orbits on the centre manifold and use the inverse change to compute quasi-periodic Halo orbits with two frequencies and quasi-periodic Lissajous orbits with three frequencies. Finally, Section 5 is devoted to conclusions and future work.

2 Normal forms for periodic time dependent Hamiltonians

This section is concerned about the generalisation of some key aspects of autonomous Hamiltonian formalism to periodic time dependent Hamiltonians. In this regard, we review the classical Lie transformation method. The idea is to introduce concepts and results that are used to develop the method. We assume that we have a Hamiltonian system, with n degrees of freedom, that depends periodically on time with period $T_H = \frac{2\pi}{\omega_H}$. A standard way of autonomizing the Hamiltonian is to add an extra degree of freedom: the time is seen as an angle Θ , and a new action I_Θ is added to keep the Hamiltonian form,

$$\bar{H} = \omega_H I_\Theta + H(Q, P, \Theta), \quad (1)$$

where (Q, P) belong to \mathbb{R}^{2n} . The main idea is to adapt a methodology that works with autonomous Hamiltonians. Although the autonomized system (1) has $n + 1$ degrees of freedom, the simplicity of the I_Θ -dependence has some consequences that we will exploit.

We assume that Hamiltonian (1) has a periodic orbit of period T_H , and that we are interested in a description of the dynamics in an extended neighbourhood of the orbit. The first step is to translate the periodic orbit to the origin so that now the origin is an equilibrium point. We expand the Hamiltonian in power series w.r.t. (Q, P) , with coefficients that depend (periodically) on Θ . When needed, we will handle these periodic coefficients as Fourier series. As we have expanded at an equilibrium point, the power expansion of the Hamiltonian starts at degree 2. In the next section we explain how to arrange the second order terms of the Hamiltonian by means of the Floquet Theorem.

2.1 The symplectic Floquet Theorem

The second degree terms of the Hamiltonian can be reduced to constant coefficients by means of the well known Floquet Theorem. The standard formulation of this theorem can be found in any elementary textbook on Differential Equations, we provide here a Hamiltonian formulation.

Theorem 2.1 (A Symplectic Floquet Theorem). *Let us consider a Hamiltonian function*

$$H = \omega_H I_\Theta + Q^T A_1(\Theta) Q + Q^T A_2(\Theta) P + P^T A_3(\Theta) P,$$

where $A_j \in \mathcal{C}^0(\mathbb{T}, M_n\mathbb{C})$, and $A_1(\Theta)$ and $A_3(\Theta)$ are symmetric matrices for all $\Theta \in \mathbb{T}$. Then, there exist a change of variables $(Q, P) \rightarrow (\bar{Q}, \bar{P})$ which is canonical, linear in (Q, P) and depends periodically on Θ , such that the transformed Hamiltonian takes the form

$$\bar{H} = \omega_H I_\Theta + \bar{Q}^T B_1 \bar{Q} + \bar{Q}^T B_2 \bar{P} + \bar{P}^T B_3 \bar{P},$$

where B_j do not depend on Θ and B_1, B_3 are symmetric matrices. We will refer to this transformation as the Floquet change of variables.

See [GJMS93] for a constructive proof of the result. Now we will discuss how to translate Theorem 2.1 into an algorithm to compute the Floquet change. Let us write the ODEs corresponding to the previous Hamiltonian in compact form,

$$\begin{cases} \dot{u} = G(\Theta)u, & u(0) = I, \\ \dot{\Theta} = \omega_H. \end{cases} \quad (2)$$

Let M be the fundamental matrix. To simplify the discussion, assume that there exist a linear change of variables that casts M into the form

$$D_M = \begin{pmatrix} \mathcal{U} & 0 & 0 \\ 0 & \mathcal{C} & 0 \\ 0 & 0 & \mathcal{S} \end{pmatrix},$$

where $\mathcal{U}, \mathcal{S} \in M_d(\mathbb{R})$ are diagonal matrices such that $[\rho(\mathcal{U})]^{-1} < 1$, $\rho(\mathcal{S}) < 1$ and $\mathcal{C} \in M_r(\mathbb{C})$ with $\text{Spec}(\mathcal{C}) \in \mathbb{S}^1 := \{z \in \mathbb{C} \text{ such that } |z| = 1\}$. To keep the discussion simple, let us also assume that all the eigenvalues have multiplicity one (all these assumptions are satisfied in the Bicircular problem). Then, we proceed as follows:

1. We compute the monodromy matrix M of (2) by numerical integration.
2. Let S be the diagonalizing transformation $M = SD_M S^{-1}$. Due to the Hamiltonian structure of the problem, the columns of S can be scaled such that

$$S^T J S = -iJ, \quad S^{-1} = -iJ S^T J,$$

where $i = \sqrt{-1}$.

3. Next we compute

- $\omega_1, \dots, \omega_r$ such that $\lambda_j^c = e^{i\omega_j T}$, $\lambda_j^c \in \text{Spec}(\mathcal{C})$,
- $\alpha_1, \dots, \alpha_d$ such that $\lambda_j^h = e^{i\alpha_j T}$, $\lambda_j^h \in \text{Spec}(\mathcal{U})$.

Note that the values ω_j are not uniquely defined. If ω_j is a complex logarithm divided by the period, then any of the values $\pm(\omega_j + \frac{2k\pi}{T})$, $k \in \mathbb{Z}$ is also admissible. Therefore, we have some freedom to choose them. Defining

$$D_B = \text{diag}(\alpha_1, \dots, \alpha_d, i\omega_1, \dots, i\omega_r, -\alpha_1, \dots, -\alpha_d, -i\omega_1, \dots, -i\omega_r),$$

and $B = SD_B S^{-1}$, we have that B is a real matrix such that $M = e^{BT}$.

4. Finally, integrating the initial value problem

$$\begin{cases} \dot{P}(\Theta) = Q(\Theta)P(\Theta) - P(\Theta)B, & P(\Theta) = I, \\ \dot{\Theta} = \omega_H, \end{cases} \quad (3)$$

we obtain the Floquet change.

Remark 2.2. *It is advisable to perform an extra change of variables that casts B into a more suitable (real) form J_B , let us explain how it is constructed. Recall that $\alpha_1, \dots, \alpha_d$ are the normalized logarithms¹ of the real eigenvalues, $\omega_1, \dots, \omega_r$ are the normalized logarithms of the complex eigenvalues and $d + r = n$. Then,*

$$J_B = \begin{pmatrix} H & E \\ -E & H \end{pmatrix},$$

where H and E are diagonal blocks of size $n \times n$. If $d \neq 0$ and $r \neq 0$, there are not enough α_j 's nor ω_j 's to fill all the entries of H and E , then the remaining entries are filled with zeros and the values are arranged so the sub-block $(H|E)$ has maximal rank. To compute J_B consider the matrix R defined in the following way: The first n columns are the eigenvectors corresponding to the unstable eigenvalues and the real parts of the eigenvectors related to complex eigenvalues. The remaining columns are filled with the eigenvectors corresponding to the real stable eigenvectors and the imaginary parts of the complex eigenvectors. The columns can be arranged and scaled so the matrix R is symplectic. We also need to compose the changes P and R . The computation of P and the subsequent composition with R can be done at the same time if we integrate the system (3) with the initial data $P_0 = R$.

Remark 2.3. *As it has been mentioned before, there is some freedom when computing the normalized logarithms of the complex eigenvalues. There is, however, a optimal choice for these logarithms. Adding multiples of the frequency of the time dependence introduces rotations in the change P . These rotations affects the size of the Fourier coefficients of P . The optimal choice is the one that makes the dominant Fourier coefficients to be at the beginning of the Fourier series. That is, we should use this freedom to make the change as close as possible to constant coefficients. In problems which are a perturbation of an autonomous one, we know in advanced that the logarithms are to be chosen as close as possible to the frequencies of the dynamical equivalent of the periodic orbit in the autonomous system.*

Let us consider J_B defined as in Remark 2.2. The associated Hamiltonian reads as

$$H_{J_B} = \sum_{j=1}^d \alpha_j q_j p_j + \frac{1}{2} \sum_{j=1}^r \omega_j (q_j^2 + p_j^2). \quad (4)$$

A Hamiltonian with expansion $H = \sum_{k \geq 0} H_k$ such that H_2 has the form (4) is said to be in real Floquet normal form. To normalize the high order terms, it is much better to have the second order terms of the Hamiltonian in complex normal form,

$$H_2 = \sum_{j=1}^d \alpha_j q_j p_j + \sum_{j=1}^r \mathbf{i} \omega_j Q_j P_j. \quad (5)$$

The change of coordinates to go from (4) to (5) is

$$q_j = \frac{Q_j + \mathbf{i} P_j}{\sqrt{2}}, \quad p_j = \frac{\mathbf{i} Q_j + P_j}{\sqrt{2}}. \quad (6)$$

It is simple to check that this is, indeed, a canonical transformation. The inverse of (6) is

$$Q_j = \frac{q_j - \mathbf{i} p_j}{\sqrt{2}}, \quad P_j = \frac{-\mathbf{i} q_j + p_j}{\sqrt{2}}. \quad (7)$$

¹By normalized, we mean that the logarithms are divided by the period T .

2.2 Higher order normal form

In this section we assume that we have a Hamiltonian expanded in power series, starting at degree 2, with coefficients that are periodic functions w.r.t. an angle Θ (the time). The terms of second degree are in complex normal form (5). Our goal is to obtain a Birkhoff normal form by means of Lie series. We will use the scheme described in [Jor99] to avoid the use of the Lie triangle. To summarise the procedure, let us recall that a Poisson bracket of two functions f and g depending on (Q, P, Θ, I_Θ) is defined as

$$\{f, g\} = \sum_{i=1}^n \left[\frac{\partial f}{\partial Q_i} \frac{\partial g}{\partial P_i} - \frac{\partial f}{\partial P_i} \frac{\partial g}{\partial Q_i} \right] + \frac{\partial f}{\partial \Theta} \frac{\partial g}{\partial I_\Theta} - \frac{\partial f}{\partial I_\Theta} \frac{\partial g}{\partial \Theta}.$$

An important property (that is easy to check) is that, if f and g do not depend on I_Θ and both are homogeneous polynomials w.r.t. (Q, P) of degrees r and s respectively, with coefficients that depend periodically on Θ , then $\{f, g\}$ is an homogeneous polynomial w.r.t. (Q, P) of degree $r + s - 2$ with coefficients that depend periodically on Θ .

The Lie series method is based on the following property. If G is a Hamiltonian system, then its time 1 flow is a canonical transformation (and, hence, it preserves the Hamiltonian form), and the composition of this time 1 flow with a Hamiltonian H can be computed as

$$H + \{H, G\} + \frac{1}{2!} \{\{H, G\}, G\} + \frac{1}{3!} \{\{\{H, G\}, G\}, G\} + \dots$$

If H is a power series expansion, and G is chosen as a polynomial, this computation can be carried out easily. The goal is to choose a suitable G (generating function) such that the Hamiltonian has the desired form. Since in our case the action I_Θ already appears in a very simple way, there is no need to modify it. Therefore, we will construct generating functions not depending on I_Θ . Hence, for some H of the form (1) and G not depending on I_Θ we have

$$\{H, G\} = \left[\frac{\partial H}{\partial Q_i} \frac{\partial G}{\partial P_i} - \frac{\partial H}{\partial P_i} \frac{\partial G}{\partial Q_i} \right] - \omega_H \frac{\partial G}{\partial \Theta}.$$

As it has been mentioned above, we start with Hamiltonian of the form $H = \omega_H I_\Theta + H_2 + H_3 + \dots$, where H_2 is in complex normal form (5) and $H_j = H_j(Q, P, \Theta)$, $j \geq 3$, is a homogeneous polynomial of degree j whose coefficients are complex valued periodic functions of Θ . The normalizing process starts by degree 3, using a generating function G_3 which is also a homogeneous polynomial of degree 3 in (Q, P) whose coefficients depend periodically on Θ . Then, we will arrange degree 4 by using a suitable G_4 , and so on.

Let us discuss how to arrange the terms of degree, say, m . So, suppose that the Hamiltonian is already in suitable form up to degree $m - 1$:

$$H = \omega_H I_\Theta + H_2(Q, P) + \sum_{j=3}^{m-1} H_j(Q, P, \Theta) + H_m(Q, P, \Theta) + H_{m+1}(Q, P, \Theta) + \dots$$

where $H_m(Q, P, \Theta) = \sum_{|k|=m} h_m^k(\Theta) Q^{k^1} P^{k^2}$, $h_m^k(\Theta) = \sum_j h_{m,j}^k e^{j\mathbf{i}\Theta}$ and $k = (k^1, k^2) \in \mathbb{Z}^3 \times \mathbb{Z}^3$ is a multi-index. We want to make a change of variables that removes some specific terms in H_m (the choice of terms to be removed will be discussed later on). Let us call G_m the generating function of the canonical transformation we are looking for,

$$G_m = G_m(q, p, \Theta) = \sum_{|k|=m} g_m^k(\Theta) Q^{k^1} P^{k^2}, \quad g_m^k(\Theta) = \sum_j g_{m,j}^k e^{j\mathbf{i}\Theta}.$$

Applying the transformation defined by the time 1 flow of Hamiltonian G_m (for details, see the Appendix A of [Jor99]), we can see that the terms of degree m of the transformed Hamiltonian, \bar{H}_m , are given by

$$\bar{H}_m = H_m + \{\omega_H I_\Theta, G_m\} + \{H_2, G_m\} \equiv H_m + \omega_H \frac{\partial G_m}{\partial \Theta} + \{H_2, G_m\}. \quad (8)$$

We define as $\eta = (\alpha_1, \dots, \alpha_d, i\omega_1, \dots, i\omega_r)$ the vector of coefficients of H_2 (see (5)). As

$$\{H_2, G_m\} = \sum_{|k|=m} \langle k^2 - k^1, \eta \rangle g_m^k(\Theta) Q^{k^1} P^{k^2},$$

we have that the transformed Hamiltonian (8) is

$$\bar{H}_m = \sum_{|k|=m} \left[h_m^k(\Theta) + \omega_H \frac{dg_m^k}{d\Theta}(\Theta) + \langle k^2 - k^1, \eta \rangle g_m^k(\Theta) \right] Q^{k^1} P^{k^2}.$$

This expression makes easy to choose periodic functions g_m^k such that \bar{H}_m has some specific form, with some limitations: if $k^1 = k^2$, it is clear that it is not possible to cancel the average of h_m^k ($k^1 = k^2$ is usually called an unavoidable resonance). In what follows, we will assume that there are no other resonances, that is, $\langle k, \eta \rangle \neq 0$ for all $k \in \mathbb{Z} \setminus \{0\}$. If we want to construct a complete normal form, then we have to remove everything except the unavoidable resonances. This is done by the generating function

$$g_m^k(\Theta) = \begin{cases} \frac{-h_{r,0}^k}{\langle \eta, k^2 - k^1 \rangle} + \sum_{j \neq 0} \frac{h_{m,j}^k}{ij\omega_H - \langle \eta, k^2 - k^1 \rangle} e^{j i \Theta}, & \text{if } k^1 \neq k^2, \\ \sum_{j \neq 0} \frac{h_{m,j}^k}{ij\omega_H} e^{j i \Theta}, & \text{if } k^1 = k^2. \end{cases}$$

The advantage of complete normal forms is that they are explicitly integrable, so the dynamics can be studied very easily. The disadvantage is that they usually have a very small radius of validity due to the effect of the so-called small divisors. Because of that, we will not perform a complete normal form but a partial one. More concretely, we focus on uncoupling the elliptic directions from the hyperbolic ones.

2.3 Centre manifold reduction

A centre manifold reduction is a seminormal form such that the transformed Hamiltonian has an invariant manifold tangent to the elliptic (centre) directions. This is achieved by cancelling some specific monomials. To simplify the explanations, let us assume that we have only one hyperbolic direction while the remaining ones are elliptical (this is indeed the case of the L_1 point). If (Q_1, P_1) are the hyperbolic directions, then we choose to suppress all the monomials such that the exponent of Q_1 is different from the exponent of P_1 . This means that the Hamiltonian depends on (Q_1, P_1) through the product $Q_1 P_1$. It is easy to check that, then, the quantity I_1 is a first integral and setting $I_1 = 0$ the Hamiltonian is reduced in one degree of freedom and restricted to the elliptic (centre) directions.

During this process of reduction, we can also suppress the time dependence of the Hamiltonian. This is what we have done for the expansion at L_1 . As it has been mentioned before,

this introduces small divisors which reduce the radius of convergence of the expansions, but it allows to study the dynamics in a much simpler way.

If the initial Hamiltonian function is analytic (which is the case of the BCP), as we are only performing a finite number of changes of variables, we can ensure that the final Hamiltonian has a finite domain of convergence.

Remark 2.4. *In [AS00, And02] Andreu and Simó use another criterion for the centre manifold. Their criterion preserves more monomials and, therefore, the radius of convergence is slightly larger. However, it does not produce additional first integrals.*

2.4 Changes of variables

We are also interested in computing explicitly the change of variables that transforms the coordinates of the normal form to synodical coordinates and vice-versa. We have followed the same scheme as in [Jor99].

The global change is split in two different sub-changes. The first one is the translation of the periodic orbit plus the linear Floquet change that puts H_2 in diagonal form (we will refer to these coordinates as “diagonal” coordinates). The second sub-change consists of the nonlinear change that goes from the normal form (or centre manifold) coordinates to the diagonal ones. Let us focus in the second sub-change.

The nonlinear change is obtained as a sequence of transformations using the generating functions G_3, G_4, \dots , used to arrange each degree. For instance, the change of variables corresponding to G_3 is obtained as follows,

$$\begin{aligned} q_i^{(3)} &= q_i + \{q_i, G_3\} + \frac{1}{2!} \{\{q_i, G_3\}, G_3\} + \dots, \\ p_i^{(3)} &= p_i + \{p_i, G_3\} + \frac{1}{2!} \{\{p_i, G_3\}, G_3\} + \dots, \end{aligned}$$

where $q_i^{(3)}, p_i^{(3)}$ denotes the series obtained in this transformation. Now we can apply G_4 ,

$$\begin{aligned} q_i^{(4)} &= q_i^{(3)} + \{q_i^{(3)}, G_4\} + \frac{1}{2!} \{\{q_i^{(3)}, G_4\}, G_4\} + \dots, \\ p_i^{(4)} &= p_i^{(3)} + \{p_i^{(3)}, G_4\} + \frac{1}{2!} \{\{p_i^{(3)}, G_4\}, G_4\} + \dots, \end{aligned}$$

and this is the transformation that goes from the normal form coordinates of degree 4 to the initial diagonal coordinates. This process can be carried out up to the desired order. To obtain the inverse change we can apply the same procedure but using $-G_3, -G_4, \dots$

2.5 Complexification and realification

During the computations, we work with Hamiltonian systems that are expanded in complex variables. This largely simplifies the computation of the normal form as the systems to be solved to find the generating functions G_j are diagonal. However, when studying the Hamiltonian reduced to the centre manifold, it is easier to work in real coordinates. Then, we perform the linear transformation (7) to the reduced Hamiltonian to obtain the final (real) reduction to the center manifold. In this last step, we have checked, as an extra test, that the imaginary part is of the order of the roundoff. Finally, this transformation (7) is also used on the changes of variables.

3 The dynamical replacement of L_1 in the BCP

The BCP is build assuming Earth and Moon to behave as in the RTBP, that is, they move following circular orbits centred in their common barycentre. At the same time, this barycentre and Sun move following another circular orbit, with Sun, around the barycentre of Earth-Moon and Sun. Notice that is this model can be seen as two coupled RTBP's. We take the units and the system of coordinates as in the Earth-Moon RTBP. With all this considerations the model, a three and a half degrees of freedom perturbation of the RTBP, has a Hamiltonian function that writes as

$$H_{BCP} = \frac{1}{2}(p_x^2 + p_y^2 + p_z^2) + yp_x - xp_y - \frac{1-\mu}{r_{PE}} - \frac{\mu}{r_{PM}} - \frac{\varepsilon m_S}{r_{PS}} - \frac{\varepsilon m_S}{a_S^2}(y \sin \theta - x \cos \theta).$$

Here the units and coordinates are taken as in the Earth-Moon RTBP, m_S is the mass of Sun, a_S the semi-major axis of Sun, $r_{PE}^2 = (x - \mu)^2 + y^2 + z^2$, $r_{PM}^2 = (x - \mu + 1)^2 + y^2 + z^2$, $r_{PS}^2 = (x - x_S)^2 + (y - y_S)^2 + z^2$, $x_S = a_S \cos \theta$, $y_S = -a_S \sin \theta$, $\theta = \omega_S t$ and ω_S is the mean angular velocity of Sun in these synodic coordinates. Notice that we have introduced an additional parameter ε establishing an homotopy between the RTBP ($\varepsilon = 0$) and the BCP ($\varepsilon = 1$). Due to the periodic perturbation due to Sun, the Lagrangian points are no longer equilibria, they are replaced by periodic orbits with the same period as Sun's ($T_S = 2\pi/\omega_S$). We name these replacements as dynamical equivalents of the Lagrangian points.

3.1 The dynamical equivalent of L_1

Our first goal is to compute the periodic orbit(s) that are born around the equilibrium points when ε goes from zero (the RTBP) to one (the BCP). Due to the high instability of L_1 , we have applied a multiple shooting technique combined with a continuation method to go from $\varepsilon = 0$ to $\varepsilon = 1$. When ε reaches 1, the replacement is a small unstable periodic orbit with the same normal behaviour as L_1 (four elliptic directions and two hyperbolic ones). The size of the orbit is around 10^{-3} and its (x, y) projection revolves L_1 twice in T_S units of time (see Figure 2). The linear normal behaviour is of type saddle \times centre \times centre. An important feature to be stressed about this orbit is its high instability.

The unstable eigenvalue of the monodromy matrix is large, around 10^8 . This implies that the dynamics near L_1 is dominated by this large eigenvalue and, in particular, initial conditions close to L_1 escape through the unstable manifold of the dynamical replacement. The reason for this large instability is that the eigenvalue of the dynamical replacement is, at first order, the exponential the eigenvalue of L_1 in the RTBP multiplied by the period of Sun. Notice that this also happens for small values of ε , that is, the large instability appears because we are measuring the eigendirections along a whole orbit of period T_S . However, there are two elliptic directions related to the periodic orbit L_1 . Some rich dynamics is to be expected due to the nonlinear terms related to the elliptic directions. For this reason we are interested in decoupling the hyperbolic and the elliptic part.

3.2 The Floquet change

Assume that the dynamical equivalent of L_1 has already been translated to the origin, and the Hamiltonian has been expanded. We recall that, under these conditions, the Hamiltonian has no terms of order one. In order to simplify the second order terms we apply a symplectic Floquet

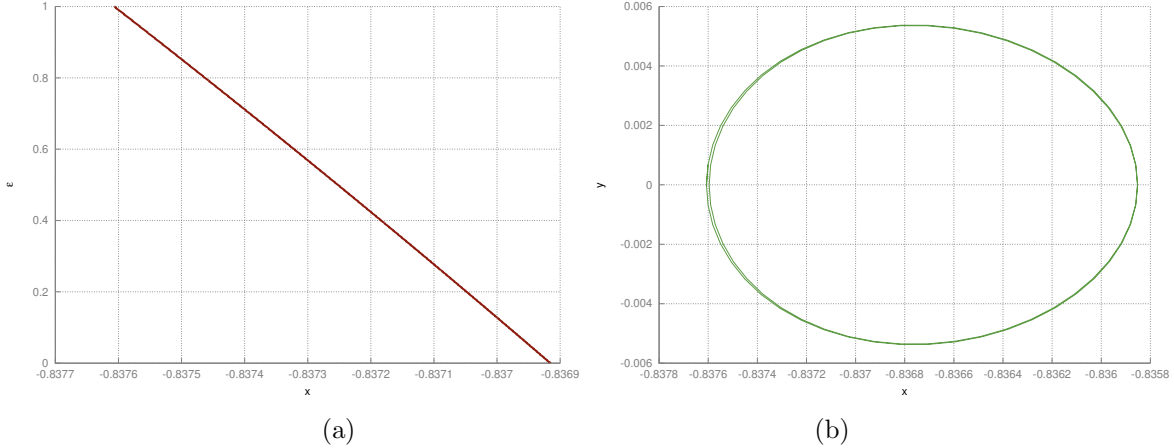


Figure 2: Left: Continuation of L_1 as T_S periodic orbit with respect to ε . Horizontal axis: x . Vertical axis: ε . Right: Dynamical replacement of L_1 . Horizontal axis x . Vertical axis y .

change of variables as explained in Section 2.1. As there is some freedom in the construction of the change, we discuss the details here. The dynamical replacement of L_1 has a single hyperbolic direction, that is, the set of eigenvalues is given by $(\lambda_h, \lambda_h^{-1}, \lambda_{e,1}, \lambda_{e,1}^{-1}, \lambda_{e,2}, \lambda_{e,2}^{-1})$. Here $|\lambda_h| \gg 1$ is the unstable eigenvalue, while $|\lambda_{e,1}| = |\lambda_{e,2}| = 1$ determine the elliptic directions.

The first question to be addressed is related to Remark 2.3. The normalized logarithms are given by

$$\alpha_1 = \log \lambda_h, \quad \omega_{1,2} = \log \lambda_{e,1,2}.$$

Here, $\omega_{1,2}$ are to be understood as a complex logarithms of the elliptic eigenvalues. As mentioned, any combination $\pm(\omega_i + k\omega_S)$ for $i = 1, 2$ and $k \in \mathbb{Z}$ is also an admissible choice. In Remark 2.3 we discuss the optimal choice for these logarithms in terms of the decay of the Fourier series representing each entry of the Floquet change. In particular, we are interested in the change of variables which is as close as possible to constant coefficients. This is obtained, in this case, selecting $\omega_1 = 2.32981963603288$ and $\omega_2 = 2.26695149158478$, which are close to the frequencies related to the equilibrium point L_1 in the RTBP (2.33438585628816 and 2.2688310655411 respectively).

We also construct the matrix R defined in Remark 2.2 by choosing the elliptic eigenvectors carefully. These can be scaled so that R has a very simple form and, in particular, the elliptic directions coincide with the axes in the final coordinates. This adds some symmetries to the expansion that can be used to get a better performance, see [Jor99]. With these considerations, the Floquet change is composed with the second order of the Hamiltonian, reducing it to real Floquet normal form, that is:

$$H_2 = \alpha_1 x p_x + \omega_1 \frac{y^2 + p_y^2}{2} + \omega_2 \frac{z^3 + p_z^3}{2}.$$

3.3 On the expansion of the Hamiltonian

Let us summarise how to expand the Hamiltonian function. Let $t \mapsto g(t) \in \mathbb{R}^6$ be the T_S -periodic orbit that replaces L_1 . We denote by g_i for $i = 1, \dots, 6$ its components. Let $\bar{\gamma}_i = \frac{1}{T_S} \int_0^{T_S} g_i(s) ds$

be the corresponding averages and let γ be the distance between Moon and the average of the periodic orbit. We will apply the three following changes:

1. A scaling by γ . This is done to get a new units such that the (averaged) distance between the periodic orbit and the Moon is equal to one. With this we assure the expansion of the Hamiltonian to have radius of convergence close to one.
2. A translation by g , to put the periodic orbits at the origin. This will leads to a Hamiltonian with no order one monomials as discussed in the previous section.
3. A Floquet symplectic change. This will put the second order of the Hamiltonian in complex diagonal form.

These three changes together define an affine transformation that will cancel the first order terms and will simplify the second order ones. Applying this affine change of variables, the Hamiltonian will take the form

$$H = \alpha_1 x p_x + \frac{\omega_1}{2}(y^2 + p_y^2) + \frac{\omega_2}{2}(z^2 + p_z^2) - \left(\frac{1-\mu}{r_{PE}} + \frac{\mu}{r_{PM}} + \frac{m_S}{r_{PS}} \right)^{[\geq 3]}.$$

Notice that the names of the variables have been kept. This is to avoid heavy notation and we hope this will cause no confusion to the reader. The main issue is, therefore, to expand the gravitational potentials of the Earth, the Moon and the Sun in these new variables. To produce the Taylor expansion of a gravitational potential is a well known problem and there are several approaches to do so. We focus on the following one: A gravitational potential can be expressed in the basis of Legendre polynomials as

$$\begin{aligned} \frac{1}{r_{pb}} &:= \frac{1}{\sqrt{(x - A(\theta))^2 + (y - B(\theta))^2 + (z - C(\theta))^2}} \\ &= \frac{1}{D(\theta)} \sum_{k \geq 0} \left(\frac{\rho}{D(\theta)} \right)^k P_k \left(\frac{A(\theta)x + B(\theta)y + C(\theta)z}{D(\theta)\rho} \right), \end{aligned}$$

where P_k is the k -th Legendre polynomial, $\rho^2 = x^2 + y^2 + z^2$, $D(\theta)^2 = A(\theta)^2 + B(\theta)^2 + C(\theta)^2$. Using the well known recurrences for the Legendre polynomials one can compute the expansion $1/r_{pb} = \sum_k T_k(x, y, z, \theta)$ by using the recurrence

$$T_{k+1} = \frac{1}{D(\theta)} \left[\frac{2n+1}{n+1} (A(\theta)x + B(\theta)y + C(\theta)z) T_k - \frac{n}{n+1} \rho^2 T_{k-1} \right],$$

with

$$T_0 = \frac{1}{D(\theta)}, \quad \text{and} \quad T_1 = \frac{A(\theta)x + B(\theta)y + C(\theta)z}{D(\theta)^3}.$$

This approach is used in the autonomous case for a number of works [Ric80, JM99] and adapted to the periodic case in [GJMS93, GJ01, And98].

4 Dynamics near L_1 in the BCP

In this section we describe the dynamics in an extended neighbourhood of the dynamical replacement of L_1 . We have already discussed the linear normal behaviour and the Floquet normal form of the periodic orbit. We will use a reduction to the centre manifold to describe the dynamics.

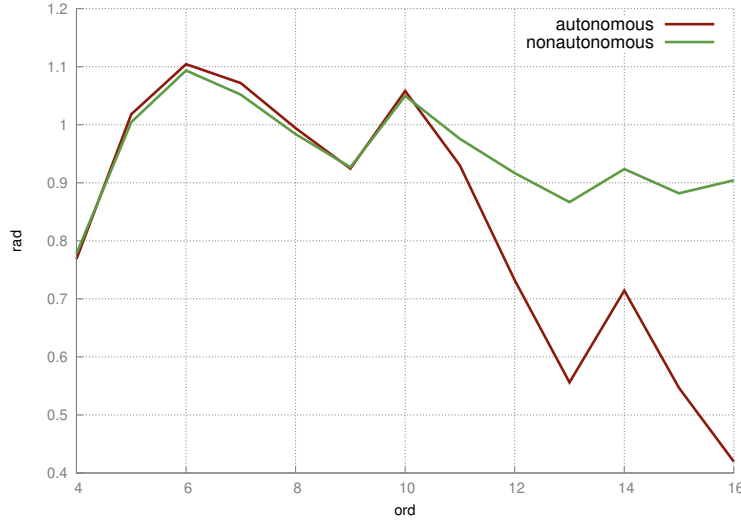


Figure 3: Estimated radius of validity of the autonomous (red) and non-autonomous (green) centre manifold w.r.t. the degree of the expansion.

4.1 Dynamics in the centre manifold

As explained in Section 2.2 we use the Lie transformation method to uncouple the hyperbolic and the elliptic parts. Recall that the generating function can also be constructed to remove the time dependence of the centre manifold. The centre manifold reduction for an autonomous Hamiltonian system with only one hyperbolic direction does not involve small divisors. On the other hand, when removing the time dependence of a non-autonomous periodic Hamiltonian, small divisors are unavoidable, and they reduce the radius of convergence of the expansion of the centre manifold. The advantage of cancelling the time dependence in the autonomous reduction to the centre manifold is that the output Hamiltonian has two degrees of freedom and, in particular, the energy is a preserved quantity. This fact can be used to reduce the problem of studying the dynamics around the periodic orbit that replaces L_1 to the study of a family of area preserving maps parameterized by the energy: Indeed, fixing the energy we only need to produce a Poincaré map by using suitable sections.

The main drawback of cancelling the time dependence is that it reduces the domain of validity of the expansions. If the size of the domain of validity is critical, then one can consider not to suppress the time dependence. For instance, we can only keep those Fourier modes that lead to small divisors in the construction of the generating function. The output system when time dependence is not removed is a Hamiltonian with two and a half degrees of freedom. Note that the analysis of the dynamics is then more involved.

We can measure the impact of small divisors on the radius of convergence of the centre manifold. A rough upper bound for the distance of the origin at which the normal form is valid can be estimated in the following way. Let us define the following quantities

$$r_n^{-1} = \sqrt[n]{\|H_n\|_1}, \quad \|H_n\|_1 = \sum_{|k|=n} |h_k|, \quad 3 \leq n \leq N.$$

This estimation is based in the root tests for power series.

In Figure 3 we display the radius of convergence of both, the Hamiltonian reduced to the centre manifold removing time dependence (purple curve) and without removing time dependence (green curve). The horizontal axis shows the order of the expansion and the vertical axis shows the estimation of the radius of convergence. We observe a similar behaviour for small degrees. At degree 10, the curves start to show different patterns. In particular, the non-autonomized centre manifold does not lose a large amount of the radius (it stays around 0.9 at order 16). The behaviour in the case is similar to the case of the autonomous case i.e. the centre manifold of the RTBP around L_1 . On the other hand, the autonomized centre manifold, has a severe decrement from degree 10. This corresponds to the encounter of small divisors in the construction of the generating function.

Notice that the Hamiltonian of the centre manifold is a power expansion depending on four variables. Indeed, the hyperbolic variables have been eliminated setting them to zero. From now on, we name q_1, p_1, q_2 and p_2 the coordinates in the normal form. Notice that the second order is in Floquet normal form and the Hamiltonian is positive definite. In fact, the frequencies have been chosen to be close to the ones of the equilibrium point L_1 in the RTBP. To do so it has been required to select a suitable value for the complex logarithm of the monodromy matrix as explained in Remark 2.3.

With this procedure we have reduced a phase-space of seven dimensions (six in phase space and one in time) to a phase-space of four dimensions. To kill time dependence, we have to pay the price of dealing with small divisors (and, hence, having a smaller domain of validity), something that does not happen in the autonomous case. Notice that each periodic orbit with the same period as Sun in the BCP is seen in the centre manifold coordinates as an equilibrium point.

Next step is to visualise the phase space of the Hamiltonian restricted to the centre manifold. As it is a two degrees of freedom Hamiltonian system, a standard strategy to visualize the dynamics of this kind of systems is to select a Poincaré spatial section and fix a level of energy to reduce the system to a family of Area Preserving Maps parametrized by the energy. We have considered, in fact, two different sections.

The first one is $\Sigma_h = \{q_2 = 0\}$. This corresponds, at first order, to fix $z = 0$ in the synodical coordinates. We will name this section as the *horizontal* one. See, in Figure 4, a representation of the phase space in the horizontal section for the values of the normalized energy fixed at $h = 0.2, 0.5, 0.7$ and 0.9 . The second section is $\Sigma_v = \{q_1 = 0\}$ and will be named *vertical* section. See in Figure 5, a representation of the phase space in the vertical section for the values of the normalized energy fixed at $h = 0.2, 0.5, 0.7$ and 0.9 .

Let us explain Figures 4 and 5. As the Hamiltonian restricted to the centre manifold is positive definite at the origin, each level of energy defines a three dimensional compact set of the phase space. When these compact sets are intersected by Σ_h and Σ_v , we obtain a two dimensional section. The periodic orbit replacing L_1 is at the origin in the centre manifold coordinates, it is totally elliptic, and has zero energy. The fixed points of both figures correspond to periodic orbits and the invariant curves to two dimensional invariant tori. In particular, the process this two Figures capture is the pitchfork bifurcation (of periodic orbits) that lead to Halo orbits (see [BB79, CPS15] for the case of the RTBP). Note that, in synodical coordinates, this corresponds to a pitchfork bifurcation of two dimensional invariant tori, giving rise to quasi-periodic Halo orbits. In Figure 4 the outer limit of the plots correspond to a planar Lyapunov orbit, and the fixed point at the centre to a vertical Lyapunov orbit. The outer limit of the plots in Figure 5 correspond to a vertical Lyapunov orbit, while the fixed point at the middle correspond to planar

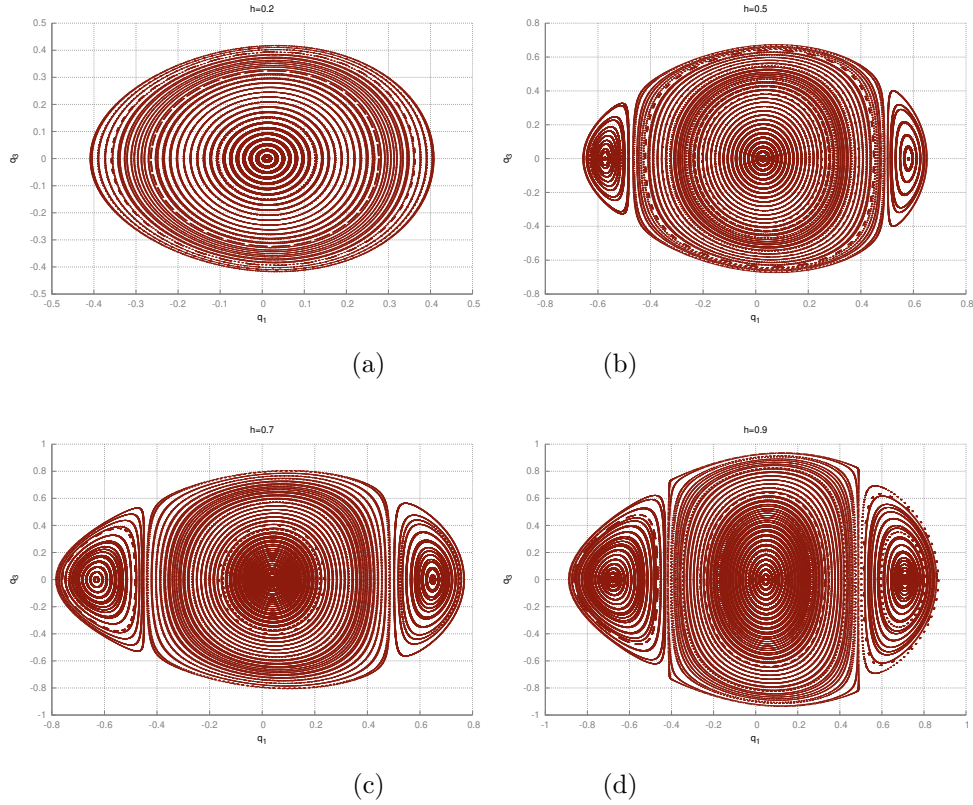


Figure 4: Horizontal section for the centre manifold of L_1 . The expansion used for the Hamiltonian is of order 12. The planar plots are obtained fixing the energy h at 0.2, 0.5, 0.7 and 0.9. Horizontal axis: q_1 . Vertical axis: q_3 . See text for more details.

Lyapunov orbits.

The translation of what we see, in Figure 4, (b), to synodic coordinates is a bifurcating family of elliptic tori appearing from the boundary of the phase-space. These tori are quasi-periodic Halo orbits. This Poincaré section allows to observe the three families of vertical invariant tori (periodic orbits in the plot) near L_1 . However, to observe the bifurcation from the boundary of the plot can be a little bit misleading. In Figure 5, the phase space the centre manifold intersected with Σ_v the bifurcation can be seen in a much better way. Here the roles of the vertical and horizontal families are switched. That is, in synodical coordinates, at each plot of Figure 5 the boundary is determined by a vertical Lyapunov torus while the invariant structure at the origin of the plots is the planar Lyapunov family of tori.

4.2 Halo and Lissajous orbits

Let us focus on Figure 4. Before the bifurcation takes place e.g. ($h = 0.2$, panel (a)), the non-chaotic motion in the Poincaré section between the origin (the periodic orbit that replaces L_1) and the vertical Lyapunov orbit is given by quasi-periodic invariant curves. These curves, when translated to synodic coordinates are quasi-periodic invariant orbits with three frequencies. This kind of orbits is known as Lissajous orbits. Notice that, in the case of the BCP, these orbits

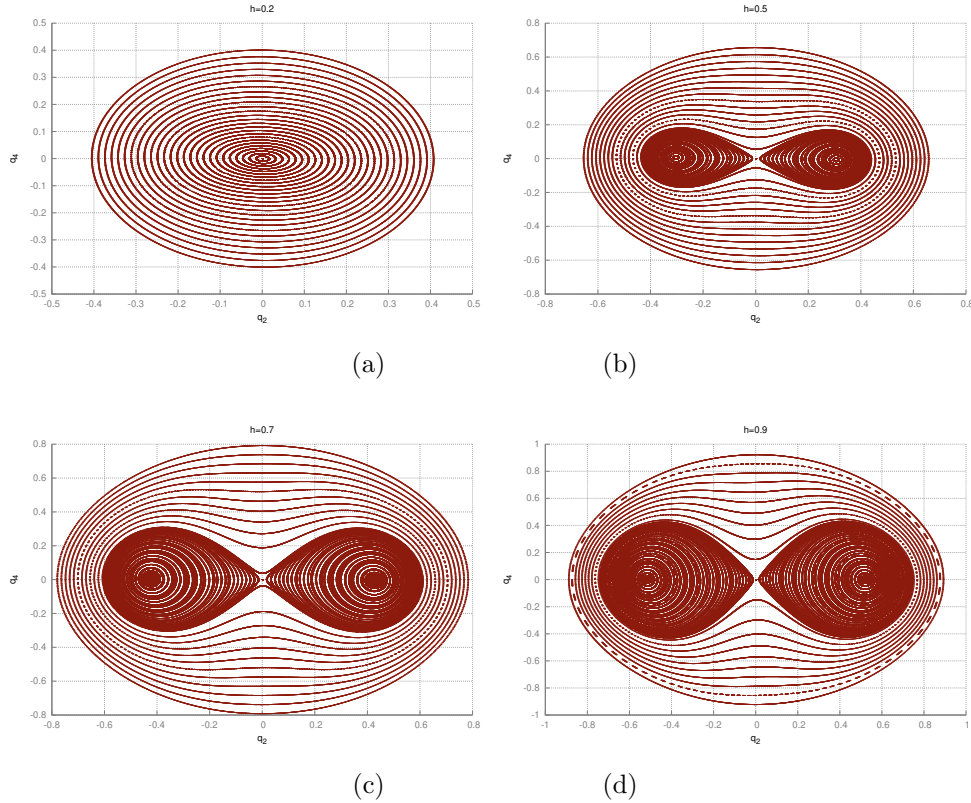


Figure 5: Vertical section for the centre manifold of L_1 . The expansion used for the Hamiltonian is of order 12. The planar plots are obtained fixing the energy h at 0.2, 0.5, 0.7 and 0.9. Horizontal axis: q_2 . Vertical axis: q_4 . See text for more details.

gain, generically, the frequency of Sun with respect to the classical ones appearing in the RTBP (see [JV97] for a general explanation). These orbits can be obtained in coordinates of the BCP simply by integrating the orbit in the centre manifold and sending the produced grid through the change of variables (constructed as explained in Section 2.4). After the bifurcation, new families appear in the Poincaré sections (e.g. Figure 4 panels (b), (c) and (d)). There appear some hyperbolic fixed points whose stable and unstable manifolds enclose regions of quasi-periodic invariant curves. These invariant curves are organized from the Halo orbits that appear as fixed points of the Poincaré map. As we have already explained, these fixed points (the Halo orbits) become two dimensional invariant tori when are sent to synodical coordinates. The other invariant curves surrounding the fixed points that give the Halo, when sent to synodical coordinates, are invariant tori with three frequencies. These orbits are known as Quasi-Halo in the case of the RTBP. Here, as in the case of Lissajous orbits, Quasi-Halo gain generically the frequency of Sun with respect to the ones appearing in the RTBP.

In Figure 6 we show a quasi-periodic Halo orbit for the energy level $h = 0.4$. In panel (a) we display the projection against the $x - y$ plane, while in panel (b) we show the projection on the $y - z$ plane. We recall that the quasi-periodic Halo orbit shown in Figure 6 is a periodic orbit in the centre manifold. Once the energy is fixed and we take a Poincaré section (horizontal or

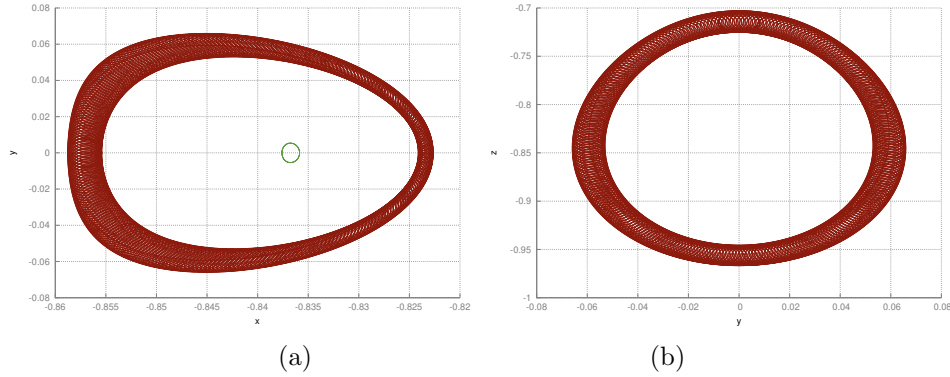


Figure 6: Quasi-periodic Halo orbit near L_1 . The point denotes the coordinates the geometrically defined L_1 and the small curve represents its dynamical replacement. (a) projection against the x - y plane. (b) projection against the y - z plane.

vertical) this Halo orbit become a fixed point. We can compute this fixed point by means of a Newton method. Then we produce a trajectory (a periodic orbit) in the centre manifold and use the change of variables to send the trajectory to synodic variables.

In Figure 7 we show an orbit lying on a three dimensional torus that correspond to a Lissajous orbit. In panel (a) we display the projection against the configuration space while, in panel (b) we show the projection against the $y - z$ plane (this is how the orbit looks like as seen from Earth). The figure is obtained as follows: First we fix the energy level $h = 0.1$ for the Hamiltonian reduced to the centre manifold. We select an initial condition close to the origin of the centre manifold. Generically, the corresponding trajectory corresponds to a two dimensional quasi-periodic trajectory. We produce the trajectory integrating this initial condition in the centre manifold. Then, the trajectory in the centre manifold is sent, by using the change of variables to synodical coordinates. As the change is periodically time dependent, the image of the two dimensional quasi-periodic trajectory is a three quasi-periodic trajectory and, again, the new frequency is the one corresponding to Sun.

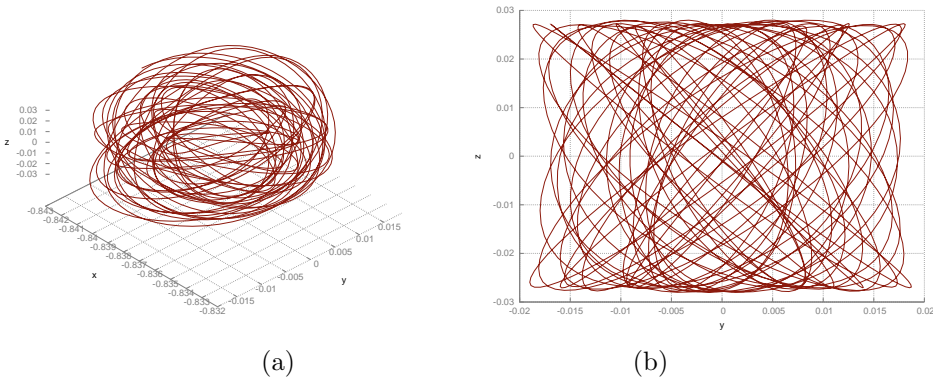


Figure 7: Lissajous tori with three frequencies near L_1 in synodic coordinates. (a) projection against the x - y - z . (b) projection against the y - z plane.

5 Conclusions and future work

In this paper we have studied the motion near the geometrically defined L_1 point of the Earth-Moon system in the Bicircular model. In this model, L_1 is no longer an equilibrium point but it is replaced by a periodic orbit with the same period as the Sun. We call this orbit the dynamical equivalent (replacement) of L_1 .

We have used an approach based in the computation of the centre manifold by means of Hamiltonian (partial) normal forms. An advantage from using the Hamiltonian approach is that time dependence can be removed facilitating the representation of the nonlinear dynamics near the dynamical equivalent of L_1 . Removing time dependence involves small divisors in the construction of the generating functions for the changes of variables. The radius of convergence of the centre manifold is smaller than in the case of the RTBP, where there are not small divisors. However, the process is good enough to show that, near the dynamical equivalent of L_1 , the structure of the phase space is similar to the one observed in the RTBP. In particular, the bifurcation that give rise the Halo orbit (well known in the RTBP) has its quasi-periodic counterpart in the BCP. The trajectories in a Poincaré section of the centre manifold can be sent back to synodic coordinates to obtain quasi-periodic invariant tori with two and three frequencies (e.g. quasi-periodic Halo orbits and Lissajous orbits with three frequencies).

There is however some further work to be done. In the first place, we have not investigated the motion near the translunar point L_2 . This is because the motion near this point is severely affected by the indirect effect of Sun's gravity on the particle. A better suited model such as the Quasi-Bicircular Problem (a coherent version of the BCP) should be used to investigate this point.

The reduction to an Area Preserving Map has been possible because we have chosen to cancel the time dependence of the Hamiltonian. Note that, in general, this could be problematic due to the effect of the small divisors. A consequence of the existence of these extra small divisors is that the radius of convergence of the reduced Hamiltonian is smaller. Notice that the reduction to the centre manifold for autonomous systems does not involve small divisors which gives large domains of validity. We would like to remark that, in the case of the centre manifold of L_1 , small divisors have not been a problem, as they appear at high order. If the radius of convergence were too small, a possible solution could be not to remove time dependence, at least completely. Indeed, one could choose to not kill the harmonics that lead to small divisors and reduce the Hamiltonian only by a degree of freedom. To visualize the reduced Hamiltonian would be harder in this case, as it would be mandatory to cope with a fourth dimensional symplectic map (the stroboscopic map associated to the reduced Hamiltonian). However, there are some cases in which it is not necessary a visualization, and, moreover there are techniques that permit us to visualize phase spaces of four dimensions.

A Appendix: Details on the implementation

In this section, we discuss the main aspects of the implementation of this methodology on a computer program. The programs have been written in ANSI C and C++ languages adapting the public domain software for the computation of normal forms presented in [Jor99]. We have also used the public domain package [FJ05] to build an efficient arithmetic of Fourier series. In general, the programs are built to be efficient allowing us to provide high order normal forms. As most of ideas used here can be found in [Jor99], we will skip some of the technical details.

We recommend the above-mentioned references for a deeper understanding of technical aspects. This section is structured as follows: First we give details on the arithmetic of Fourier-Taylor series, second we comment some aspects on the implementation of the Floquet change. The third point to be addressed is the implementation of the main algorithm and, finally, we discuss some tests on the software.

A.1 On Taylor-Fourier series

Here, Fourier series have complex coefficients and, hence, there are four different arithmetics nested in each operation between two homogeneous polynomials, that is

$$(1) \text{ Real} \mapsto (2) \text{ Complex} \mapsto (3) \text{ Fourier Series} \mapsto (4) \text{ Homogeneous Polynomials.}$$

In order to have a good performance the basic operations between the mathematical objects involved are to be written as efficiently as possible.

A.1.1 The arithmetic of Fourier Series

Let $f \in \mathcal{C}^\omega(\mathbb{T}, \mathbb{C})$. The Fourier coefficients of f are defined as

$$C_k = \frac{1}{2\pi} \int_{\mathbb{T}} f(s) \exp(-\mathbf{i}ks) ds.$$

In the strong regularity condition we are assuming, it is well known that the sequence of partial sums,

$$P_N(\theta) = \sum_{|k| < N} C_k \exp(\mathbf{i}k\theta),$$

converges, uniformly in θ when $N \rightarrow \infty$, to f . Moreover, if f is real analytic, the sequence $\{|C_k|\}_{k \in \mathbb{Z}}$ converges to zero exponentially i.e. there exist positive constants M and ρ such that

$$|C_k| \leq M \exp(-|k|\rho).$$

The constants M and ρ depend on f and, in particular, ρ is bounded by the distance of the closest singularity of f (regarded as a holomorphic function) to the real line. If ρ is not too small, the fast decay of the sequence $\{|C_k|\}_{k \in \mathbb{Z}}$ results in the fact that just a few coefficients are needed to describe the function f with a prescribed accuracy. When f is real-valued, it holds that $C_{-k} = \bar{C}_k$, in that case, only half of the coefficients are needed to evaluate the function. A periodic function can be stored in a computer as a finite mesh of points or as a finite set of coefficients. Let us fix a truncation order N , E_N is defined as the space of trigonometric polynomials of degree N , $M = (2N + 1)$ and $P_M = \{z = (z_1, \dots, z_M) \in \mathbb{C}^M\}$. It is trivial to see that, both, E_N and P_M are \mathbb{C} vector spaces of dimension M . The Discrete Fourier transform, $\Gamma_N : P_M \mapsto E_N$, is given by $\Gamma_N(z) = C$, where

$$C_k = \frac{1}{N} \sum_{j=0}^{N-1} z_j \exp\left(-\mathbf{i}k \frac{j}{N}\right),$$

is an isomorphism and its inverse map Γ_N^{-1} is given by $\Gamma_N^{-1}(C) = z$, where

$$z_k = \frac{1}{N} \sum_{j=0}^{N-1} C_j \exp\left(\mathbf{i}k \frac{j}{N}\right),$$

There is an excellent public package by Frigo and Johnson [FJ05] for these operations. The periodic functions are stored in a structure of the form

```
typedef struct{
    int N;
    double complex *C;
    char mvc;
} sf;
```

The integer indicates the truncation order, the vector of complex numbers contains the coefficients or the mesh of points and the char is a control parameter that encodes whether the array contains points a table of values or Fourier coefficients of the function. The point of this structure is that some operations are suited to be done with the table of values of the function, namely the elementary operations (products, divisions, square roots, etc.) and other are better suited to be performed with the Fourier coefficients, for instance, derivatives, evaluations and norms. Two key functions of the arithmetic are the ones that apply the Fourier transform (or its inverse) if it is required. The direct transformation receives an object of type `sf`, checks the control character `mvc`. In case the array `C` contains points of the table of values, it applies the Fast Fourier Transform on the object and switches the control character, otherwise, it does nothing.

Each operation of the arithmetic is to be performed over coefficients or values, hence, the first step is to transform between coefficients and values conveniently. After the transformation, the operation is done and the control character of the output is set. This prevents the program to operate objects with different control characters. This is particularly important in operations like the sum, that can be implemented in the same way no matter if the vector contains points or coefficients. In these special operations, we choose to transform the inputs into points as most of the operations have to be performed over the table of values. In general, the arithmetic is designed to perform the least possible number of transformations. In this way, any operation between Fourier Series requires (order of) $N \log N$ operations with complex numbers if previous transformations are required and (order of) N operations with complex numbers if no previous transformation is applied.

A.1.2 Handling Homogeneous Polynomials

The arithmetic of Fourier series is combined with an arithmetic that operates with homogeneous polynomials. We have used the one presented in [Jor99] and here we summarise the main ideas involved. A homogeneous polynomial of degree k in the variables (x_1, \dots, x_m) is an expression

$$P_j = \sum_{|k|=j} p_k x^k,$$

where, as usual, $k \in \mathbb{Z}_+^m$, $|k| = k_1 + \dots + k_m$, $x^k = x_1^{k_1} \cdot x_2^{k_2} \cdot \dots \cdot x_m^{k_m}$ and $p_k \in \mathbb{C}$. A homogeneous polynomial of degree j has $\psi_m(j)$ coefficients, where

$$\psi_m(j) = \sum_{i=0}^j \psi_{m-1}(i) = \binom{j+m-1}{m-1}.$$

An homogeneous polynomial of degree j and m variables is stored inside an array of $\psi_m(k)$ components (of type `sf`, see Section A.1.1). The position of the coefficients inside the array depends on the multiindex k . The relation between the position and the multiindex is handled by suitable hash functions. Using these functions, it is straightforward to write the different operations required for the previous algorithms.

A.2 On the implementation of the Floquet transformation

The computations in this part of the program are performed in extended accuracy. This is done for several reasons that shall be pointed out during the discussion. We use the `mpfr` [FHL⁺07] arithmetic and the library `mpreal` [Hol18] to overload the standard double precision arithmetic. The language `C++` is used for that purpose.

The first step is to refine the periodic orbit that replaces L_1 with extended precision. The eigenvalues and the eigenvectors of the monodromy matrix are computed and, with these, we are able to construct the real reduced Floquet matrix B (see Section 2.1). On the other, we construct the change R that casts B into real normal form J_B and compute it by evaluating $R^{-1}BR$. Notice that there is no need to compute J_B after computing the diagonal normalized logarithm as we know the entries of J_B . However, doing it in this way permits to test the transformation R . We also perform other tests during the computation such as the symplecticity of the matrices involved. If any of these tests is not passed, the program stops with a suitable message. All these extra checks are done because the outputs of the function that computes the eigenvalues sorts them according to their modulus. In principle we do not know in advance if there will be real eigenvalues or not, therefore, at each run of the program, we have to select an order for the eigenvalues to perform the subsequent computations.

Once the change R and the normal form J_B are obtained, we proceed to integrate equation (3) and the variational equation together, to obtain the Floquet transformation. These integrations are done together so we can produce coherent meshes of the periodic orbit and the periodic change of variables. As the dynamics around the periodic orbit is largely unstable and the accumulation of errors is severe, the use of extended accuracy is justified.

By this stage of the process, we have computed a tabulation of the periodic orbit and the change of variables. We do an extra computation: We perform a Fast Fourier Transform (using our own implementation) and check the leading harmonics of each entry of the change of variables, this is printed together with the output. If the produced change is not close enough to constant coefficients, we rerun the program using another choice for the normalized logarithms of the eigenvalues.

There are several parts of this program that could be implemented in a more efficient manner. For instance, the multiple accuracy could be avoided by using a multiple shooting strategy. However, as a few integrations (taking into account the refinement of the initial data) are required, the loss of efficiency is not critical in terms of computing time. For the numerical integrations with extended precision we have used a Taylor method ([JZ05]), which is very efficient for extended precision calculations. After a successful run of this program, we end up with a tabulation of the periodic orbit and the Floquet change with more than 16 correct digits. Multiple accuracy shall not be used in the subsequent computations.

A.3 Testing the software

The main test is based on the behaviour of the remainder (see [Jor99] for more details). The idea is the following: choose an initial condition in the centre manifold coordinates at a distance, say, h from the origin. Perform a few steps of a numerical integration (we have used a Runge-Kutta-Fehlberg 7(8)) and send these points by means of the change of variables to the initial synodical coordinates. Then, compute the difference of this orbit with the one obtained by direct numerical integration of the BCP in synodical coordinates. Of course, the integration has to be short due to the high instability of the orbit. We perform this computation for several values of h , and we look at the behaviour of the difference between the two orbits as a function of h . If everything is correct, this difference has to behave as h^{m+1} , where m is the truncation order of the flow. We have used this test for different values of m , and it has been passed successfully in all the cases.

Conflict of Interest: The authors declare that they have no conflict of interest.

References

- [And98] M.A. Andreu. *The quasi-bicircular problem*. PhD thesis, Univ. Barcelona, 1998.
- [And02] M.A. Andreu. Dynamics in the center manifold around L_2 in the quasi-bicircular problem. *Celestial Mech.*, 84(2):105–133, 2002.
- [AS00] M.A. Andreu and C. Simó. The quasi-bicircular problem for the Earth-Moon-Sun parameters. Preprint, 2000.
- [BB79] J. V. Breakwell and J. V. Brown. The ‘Halo’ family of 3-dimensional periodic orbits in the Earth-Moon restricted 3-body problem. *Celestial mechanics*, 20(4):389–404, Nov 1979.
- [BMGLD17] B. L. Bihan, J. J. Masdemont, G. Gómez, and S Lizy-Destrez. Invariant manifolds of a non-autonomous quasi-bicircular problem computed via the parameterization method. *Nonlinearity*, 30(8):3040, 2017.
- [CJ00] E. Castellà and À. Jorba. On the vertical families of two-dimensional tori near the triangular points of the Bicircular problem. *Celestial Mech.*, 76(1):35–54, 2000.
- [CPS15] A. Celletti, G. Pucacco, and D. Stella. Lissajous and halo orbits in the restricted three-body problem. *Journal of Nonlinear Science*, 25(2):343–370, Apr 2015.
- [CRR64] J. Cronin, P.B. Richards, and L.H. Russell. Some periodic solutions of a four-body problem. *Icarus*, 3:423–428, 1964.
- [FHL⁺07] L. Fousse, G. Hanrot, V. Lefèvre, P. Pélicier, and P. Zimmermann. Mpf: A multiple-precision binary floating-point library with correct rounding. *ACM Trans. Math. Softw.*, 33(2), June 2007.
- [FJ05] M. Frigo and S.G. Johnson. The design and implementation of FFTW3. *Proceedings of the IEEE*, 93:216 – 231, 03 2005.

- [FJ10] A. Farrés and À. Jorba. On the high order approximation of the centre manifold for ODEs. *Discrete Contin. Dyn. Syst. Ser. B*, 14(3):977–1000, 2010.
- [GDF⁺89] A. Giorgilli, A. Delshams, E. Fontich, L. Galgani, and C. Simó. Effective stability for a Hamiltonian system near an elliptic equilibrium point, with an application to the restricted three body problem. *J. Differential Equations*, 77:167–198, 1989.
- [GG78] A. Giorgilli and L. Galgani. Formal integrals for an autonomous Hamiltonian system near an equilibrium point. *Celestial Mech.*, 17:267–280, 1978.
- [GG85] A. Giorgilli and L. Galgani. Rigorous estimates for the series expansions of Hamiltonian perturbation theory. *Celestial Mech.*, 37:95–112, 1985.
- [GJ01] F. Gabern and À. Jorba. A restricted four-body model for the dynamics near the Lagrangian points of the Sun-Jupiter system. *Discrete Contin. Dyn. Syst. Ser. B*, 1(2):143–182, 2001.
- [GJ05] F. Gabern and À. Jorba. Effective computation of the dynamics around a two-dimensional torus of a Hamiltonian system. *J. Nonlinear Sci.*, 15(3), 2005.
- [GJL05] F. Gabern, À. Jorba, and U. Locatelli. On the construction of the Kolmogorov normal form for the Trojan asteroids. *Nonlinearity*, 18(4):1705–1734, 2005.
- [GJMS91] G. Gómez, À. Jorba, J. Masdemont, and C. Simó. Study refinement of semi-analytical Halo orbit theory. ESOC contract 8625/89/D/MD(SC), final report, European Space Agency, 1991. Reprinted as *Dynamics and mission design near libration points. Vol. III, Advanced methods for collinear points*, volume 4 of World Scientific Monograph Series in Mathematics, 2001.
- [GJMS93] G. Gómez, À. Jorba, J. Masdemont, and C. Simó. Study of Poincaré maps for orbits near Lagrangian points. ESOC contract 9711/91/D/IM(SC), final report, European Space Agency, 1993. Reprinted as *Dynamics and mission design near libration points. Vol. IV, Advanced methods for triangular points*, volume 5 of World Scientific Monograph Series in Mathematics, 2001.
- [Hol18] P. Holoborodko. MPFR C++. <http://www.holoborodko.com/pavel/mpfr/>, 2008-2018.
- [Hua60] S.S. Huang. Very restricted four-body problem. Technical note TN D-501, Goddard Space Flight Center, NASA, 1960.
- [JM99] À. Jorba and J. Masdemont. Dynamics in the centre manifold of the collinear points of the Restricted Three Body Problem. *Phys. D*, 132:189–213, 1999.
- [Jor99] À. Jorba. A methodology for the numerical computation of normal forms, centre manifolds and first integrals of Hamiltonian systems. *Exp. Math.*, 8(2):155–195, 1999.
- [Jor00] À. Jorba. A numerical study on the existence of stable motions near the triangular points of the real Earth-Moon system. *Astron. Astrophys.*, 364(1):327–338, 2000.

- [JS94] À. Jorba and C. Simó. Effective stability for periodically perturbed Hamiltonian systems. In J. Seimenis, editor, *Hamiltonian Mechanics: Integrability and Chaotic Behaviour*, volume 331 of *NATO Adv. Sci. Inst. Ser. B Phys.*, pages 245–252. Held in Toruń, Poland, 28 June–2 July 1993. Plenum, New York, 1994.
- [JV97] À. Jorba and J. Villanueva. On the persistence of lower dimensional invariant tori under quasi-periodic perturbations. *J. Nonlinear Sci.*, 7:427–473, 1997.
- [JZ05] À. Jorba and M. Zou. A software package for the numerical integration of ODEs by means of high-order Taylor methods. *Exp. Math.*, 14(1):99–117, 2005.
- [Ric80] D.L. Richardson. A note on a Lagrangian formulation for motion about the collinear points. *Celestial Mech.*, 22(3):231–236, 1980.
- [SGJM95] C. Simó, G. Gómez, À. Jorba, and J. Masdemont. The Bicircular model near the triangular libration points of the RTBP. In A.E. Roy and B.A. Steves, editors, *From Newton to Chaos*, pages 343–370, New York, 1995. Plenum Press.
- [Sim89] C. Simó. Estabilitat de sistemes Hamiltonians. *Mem. Real Acad. Cienc. Artes Barcelona*, 48(7):303–348, 1989.
- [Sim96] C. Simó. Effective computations in Hamiltonian dynamics. In *Mécanique céleste*, volume 1996 of *SMF Journ. Annu.*, page 23. Soc. Math. France, Paris, 1996.
- [Sim98] C. Simó. Effective computations in celestial mechanics and astrodynamics. In V.V. Rumyantsev and A.V. Karapetyan, editors, *Modern Methods of Analytical Mechanics and their Applications*, volume 387 of *CISM Courses and Lectures*. Springer Verlag, 1998.